IEEE Access
Multidisciplinary | Rapid Review | Open Access Journal

Received October 14, 2021, accepted November 1, 2021, date of publication November 8, 2021, date of current version November 12, 2021.

Digital Object Identifier 10.1109/ACCESS.2021.3125775

On the Modeling of Microstrip Lines Loaded With Dumbbell Defect-Ground-Structure (DB-DGS) and Folded DB-DGS Resonators

LIJUAN SU[1], (Member, IEEE), JONATHAN MUÑOZ-ENANO[1], (Member, IEEE), PARIS VÉLEZ[1], (Senior Member, IEEE), JESÚS MARTEL[2], (Senior Member, IEEE), FRANCISCO MEDINA[2], (Fellow, IEEE), AND FERRAN MARTÍN[1], (Fellow, IEEE)

[1]GEMMA/CIMITEC, Departament d'Enginyeria Electrònica, Universitat Autònoma de Barcelona, 08193 Bellaterra, Spain
[2]Grupo de Microondas, Universidad de Sevilla, 41012 Sevilla, Spain

Corresponding author: Ferran Martín (ferran.martin@uab.es)

This work was supported in part by the Ministerio de Economía y Competitividad (MINECO)-Spain under Project PID2019-103904RB-I00, in part by the Generalitat de Catalunya under Project 2017SGR-1159, in part by the Institució Catalana de Recerca i Estudis Avançats (who awarded Ferran Martín), and in part by the Fondo Europeo de Desarrollo Regional (FEDER) funds. The work of Lijuan Su and Paris Vélez was supported by the Juan de la Cierva Program under Project IJCI-2017-31339 and Project IJC2019-040786-I. The work of Jonathan Muñoz-Enano was supported by the Secreteraria d'Universitats i Recerca (Gen. Cat.) and European Social Fund for the Formació d'Investigadors (FI) grant.

ABSTRACT This paper presents a lumped-element equivalent circuit model of microstrip lines loaded with dumbbell defect-ground-structure (DB-DGS) resonators, etched in the ground plane. The model is valid for ordinary (i.e., unfolded) DB-DGSs, as well as for folded DB-DGSs with an arbitrary aperture angle and relative orientation between the line and the resonator. It is shown that in folded, or partially folded, DB-DGS resonators both magnetic and electric coupling between the line and the resonator should be considered, except for a particular DB-DGS orientation, namely, the one where the symmetry plane of the particle (a magnetic wall) is orthogonal to the line axis. In this case, the particle is exclusively excited by the electric field generated by the line. It is also shown that the circuit model of a microstrip line loaded with an unfolded DB-DGS resonator transversally oriented to the line can be derived from the general model by considering the effects of opening the particle, i.e., a reduction of the electric coupling. In the extreme situation where the DB-DGS is completely opened (unfolded), the electric coupling vanishes, and the particle is exclusively driven by the magnetic field generated by the line. This effect is taken into account in the model by considering that the capacitance between the line and the inner metallic region of the folded, or partially folded, DB-DGS depends on the aperture angle of the particle, and it is null when the particle is unfolded. The models are validated by parameter extraction and comparison of the circuit responses with the responses inferred by electromagnetic simulation and measurement.

INDEX TERMS Dumbbell DGS (DB-DGS), defect ground structures (DGS), folded DB-DGS, mixed coupling, microstrip technology, parameter extraction.

I. INTRODUCTION

Defect-ground-structure (DGS) resonators are slot (or aperture) resonators etched in the ground plane of planar transmission lines, typically, microstrip lines [1]–[3]. There are many types of DGS resonators, including the slot resonator (linear or circular) [4], the complementary split ring resonator (CSRR) [5], the complementary spiral resonator [6], [7] the S-shaped CSRR [8], the magnetic LC resonator [9], [10] or the dumbbell defect-ground-structure (DB-DGS) resonator [1], [11], among others. These DGS resonant elements have been used in a wide variety of applications. Examples include the implementation of microwave circuits and filters with reduced size and superior performance (exploiting the small electrical size and specific electromagnetic properties of the considered DGS resonators) [11]–[23], as well as planar antennas [24]–[27]. DGS resonators are also very interesting for the design of highly sensitive microwave

The associate editor coordinating the review of this manuscript and approving it for publication was Jenny Mahoney.

sensors, mainly, although not exclusively, devoted to permittivity measurements and characterization of material properties [28]–[36]. Resonant sensors exhibit high sensitivities to variations in the complex permittivity of the material surrounding it. Moreover, DGS-based sensors present a significant advantage as compared to sensors implemented by means of metallic sensing elements, i.e., isolation of the material under test (MUT) from the host line [37]. Specifically, in microstrip sensors based on DGS sensing resonators, the MUT should be placed in the backside of the substrate, in contact with the DGS. Therefore, the MUT is backside isolated from the line, due to the presence of the ground plane, only altered by the etched DGS resonator. It should also be indicated that such backside isolation of the MUT is especially important in microfluidic sensors [28], [34], [36], since the fluidic channel plus the necessary mechanical accessories, present also in the backside of the substrate, do not perturb the electromagnetic field generated by the line.

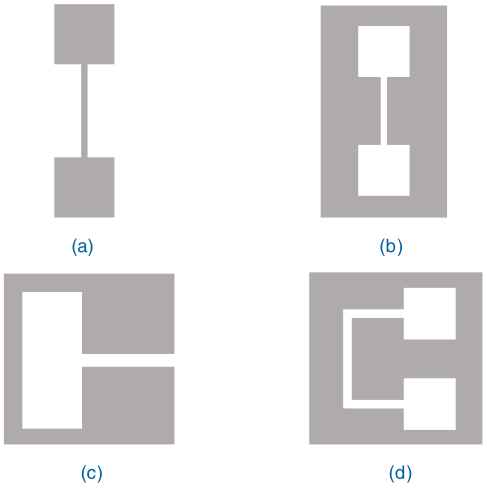

FIGURE 1. Typical topology of a SIR (a), DB-DGS (b), folded SIR (c) and folded DB-DGS (d) resonator. The metallic regions are depicted in grey.

According to the preceding paragraph, it is clear that DGS resonators are of high interest in microwave engineering. Among them, the so-called dumbbell DGS (DB-DGS) resonator [1], [11], [13], [19], the complementary (or dual) counterpart of the step impedance resonator (SIR) [38], [39] (see Fig. 1), has been exhaustively used in the design of circuits, filters, and sensors. For example, DB-DGS resonators have been applied to the suppression of common-mode noise in microstrip differential lines [40]. DB-DGS resonators are also of interest for the implementation of stopband filters, by virtue of the notched response of a DB-DGS-loaded microstrip line [13], [20]. Finally, let us mention that the achievable sensitivities in DB-DGS-based frequency-variation sensors are superior to those that can be obtained in other DGS-based sensors, as recently reported in [35]. A variant of the DB-DGS resonator is the folded DB-DGS resonator, the dual counterpart of the folded SIR (see Fig. 1). These folded particles may be of interest in certain applications involving inter-resonator's coupling (for example, filters based on coupled folded SIRs [41] and coupled folded DB-DGSs [21], [22] have been proposed). Also, depending on the length of the narrow slot of the DB-DGS particle, its shape factor might be too extreme, unless it is folded.

DGS resonators, including DB-DGS and folded DB-DGS resonators, are preferentially combined with microstrip lines, by etching them in the ground plane, beneath the line. By this means, the resonant particle is under the influence of the electromagnetic field generated by the line, a necessary condition to excite the particle and obtain the desired functionality. However, for the design of microwave circuits or sensors based on microstrip lines loaded with DB-DGSs or with folded DB-DGSs, accurate circuit models are needed. Like the SIR resonator, the DB-DGS resonator (ordinary or folded) can be considered to be electrically small, by virtue of the high contrast between the width of the narrow (central) slot and the width of the apertures at the extremes. Therefore, a microstrip line loaded with a DB-DGS or a folded DB-DGS resonator can be described by means of a lumped element circuit model consisting of reactive elements and, eventually, with electric and/or magnetic couplings (obviously, the effects of losses can be accounted for by introducing resistances in the model, although this aspect is not considered in this paper).

The model of a microstrip line loaded with an ordinary (unfolded) DB-DGS resonator transversally oriented has been reported in the literature, and it consists of a parallel resonant tank series-connected to the line [1], [11], [42]. However, by folding the resonator, the reported model is completely different (even the topology, as shown in Fig. 1), since there is a capacitive effect between the line and the inner metallic region of the resonator, which must be included in the model. In this paper, a single model able to describe these two extreme cases (folded and unfolded DB-DGS), as well as the general case of a line loaded with a partially folded DB-DGS is proposed. This is achieved by introducing a capacitance in the model that depends on the folding level of the resonant element, being null for the ordinary (unfolded) resonator [Fig. 1(b)], maximum for the completely folded DB-DGS resonator [Fig. 1(d)], and taking intermediate values for resonators partially folded. The transition from the circuit model accounting for the response of the folded version to the circuit model corresponding to the regular unfolded one is not obvious, and constitutes the main contribution of the present paper. Additionally, the model is able to describe the structure when the folded DB-DGS resonator is rotated 90°.

The paper is organized as follows. In section II, the proposed model for a DB-DGS-loaded microstrip line is presented, and it is particularized to specific (canonical) cases, i.e., unfolded DB-DGS resonator, and folded DB-DGS resonator with transverse and longitudinal orientation. Model validation, by comparing the circuit response with extracted parameters and the response inferred from electromagnetic simulation and measurement is presented in section III.

Section IV discusses some interesting aspects related to the elements of the model. Finally, the main conclusions are highlighted in section V.

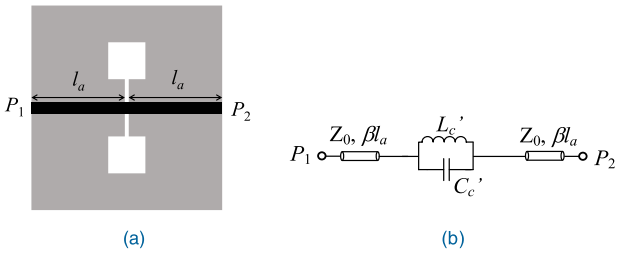

FIGURE 2. Typical topology (a) and circuit model (b) of a microstrip line loaded with a transversally oriented DB-DGS resonator. The microstrip central line is in black color, whereas the metallization of the ground plane is depicted in grey.

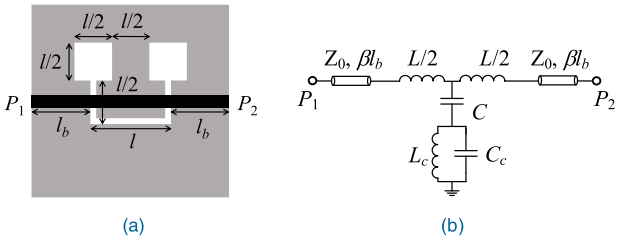

FIGURE 3. Typical topology (a) and circuit model (b) of a microstrip line loaded with a folded DB-DGS resonator oriented with the symmetry plane orthogonal to the line axis.

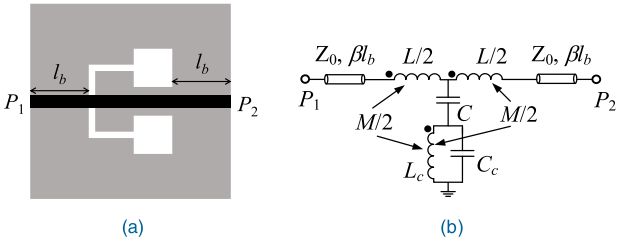

FIGURE 4. Typical topology (a) and circuit model (b) of a microstrip line loaded with a folded DB-DGS resonator oriented with the symmetry plane aligned with the line axis.

II. CIRCUIT MODEL OF A MICROSTRIP LINE LOADED WITH A DB-DGS RESONATOR WITH ARBITRARY ORIENTATION AND FOLDING LEVEL

The canonical topologies and circuit models of DB-DGS-loaded microstrip lines are depicted in Figs. 2, 3 and 4. In Fig. 2(a), the DB-DGS is unfolded and transversally oriented with regard to the line axis. The circuit model, as reported in the literature [1], [11], [42], consists of a parallel resonant tank, series connected to the line. By contrast, in the structures of Figs. 3 and 4, the DB-DGS resonator is folded. However, in Fig. 3, the symmetry plane of the resonant particle is transversally oriented to the line, whereas it coincides with the line axis in Fig. 4 (the difference is that one particle is rotated 90° with regard to the other). The folded DB-DGS resonator exhibits an electric dipole moment in the direction orthogonal to the plane of the particle at the fundamental resonance, and a magnetic dipole moment orthogonal to the symmetry plane, a magnetic wall. Therefore, the folded DB-DGS resonator can be excited either by a vertical time-varying electric field, or by a time-varying magnetic field applied in the normal direction to its plane of symmetry. Therefore, with the orientation shown in Fig. 3, the particle can only be excited by means of the electric field generated by the line, with a significant component in the vertical direction, but not with the magnetic field (note that the microstrip line supports a quasi-TEM mode with a negligible component of the magnetic field orthogonal to the symmetry plane of the DB-DGS resonator). However, by rotating the particle 90° (Fig. 4), the symmetry plane of the resonator is perfectly aligned with the symmetry plane of the line, also a magnetic wall, and the particle is excited by both the magnetic and the electric field generated by the line (mixed coupling). This mixed coupling has been also reported in reference to CSRR-loaded microstrip lines [43] (indeed, the coupling mechanisms in CSRR and folded DB-DGS resonators are similar).

According to the previous words, the circuit models of the microstrip line loaded with the folded DB-DGS resonators for both orientations are those depicted in Figs. 3(b) and 4(b). In the circuit of Fig. 3(b), L and C are the inductance and capacitance, respectively, of the line section on top of the folded resonator, with inductance L_c (mainly related to the apertures) and capacitance C_c (mostly determined by the central slot). The capacitor C accounts for the electric coupling between the line and the resonant element, the single coupling mechanism for the DB-DGS orientation of Fig. 3. In the circuit of Fig. 4(b), electric coupling is preserved. However, magnetic coupling between the line and the resonator should arise, and such coupling is accounted for by means of the mutual inductances, designated as $M/2$. By rotating the folded DB-DGS 90°, it is expected that the reactive elements of the circuit of Fig. 3(b) do not change appreciably, except L_c (obviously, provided the DB-DGS dimensions and substrate are identical in both cases). The reason is that the current path between the inner and the outer region of the folded DB-DGS might be influenced by the presence of the line strip on top of the particle. Consequently, the parameters L, C and C_c extracted from the circuit of Fig. 3(b) are assumed to be valid in the circuit of Fig. 4(b). The mutual inductance, M, and the new L_c value of the rotated resonator can be inferred by curve fitting the electromagnetically simulated (or measured) response of the structure of Fig. 4(a) (an aspect to be discussed later).

Let us now consider the DB-DGS orientation of Fig. 4, but with the resonator partially folded, see Fig. 5, as given by the angle of aperture, θ (note that for the extreme cases of $\theta = 0°$ and $\theta = 90°$, the resulting DB-DGS topology is the one of the folded and ordinary –unfolded– resonator, respectively). As far as $0 \leq \theta < 90°$, the particle exhibits an electric dipole in the vertical direction and therefore it can be electrically excited by the line. Nevertheless, the electric coupling should

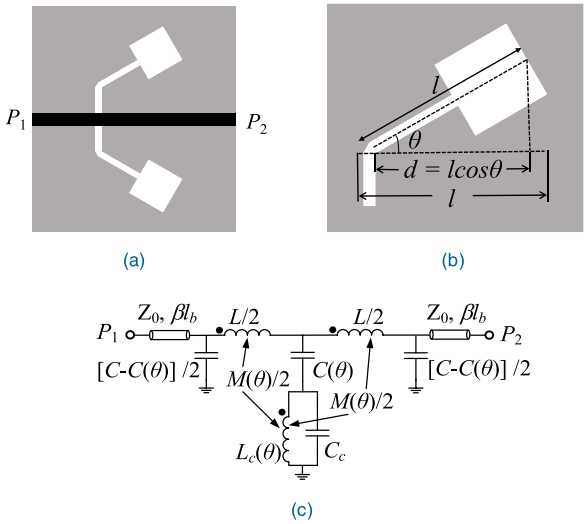

FIGURE 5. Topology of a microstrip line loaded with a folded DB-DGS resonator with an arbitrary angle of aperture (a), zoom view of the aperture arm (b), and equivalent circuit model valid for any arbitrary angle of aperture (c).

decrease as the angle of aperture increases, and such coupling must vanish for $\theta = 90°$. This dependence of the electric coupling with the angle can be taken into account by means of an angle-dependent coupling capacitance, $C(\theta)$. Reasonably, such capacitance can be considered to be the capacitance of the line section of length d corresponding to the projection of the extension of the particle in the line axis [see Fig. 5(b)]. If C is the capacitance when $\theta = 0°$, it follows that the angle-dependent coupling capacitance is simply

$$C(\theta) = C_{\text{pul}} \cdot d = C \cdot \cos(\theta) \tag{1}$$

provided $d = l \cdot \cos\theta$ and $C = C_{\text{pul}} \cdot l$, where C_{pul} is the per-unit length capacitance of the line.

On the other hand, if the model of the structure must describe the resonant element plus the line section of length l, the decrease in the capacitance C caused by the angle of aperture should be compensated by a pair of capacitances, corresponding to the line portions of length $(l - d)/2$ outside the area of influence of the DB-DGS, see Fig. 5. Obviously, such capacitances are simply $[C - C(\theta)]/2$, and are directly connected to ground in the circuit model. Note that with the considered DB-DGS orientation of Fig. 5, the magnetic coupling between the line and the DB-DGS resonator is preserved, regardless of the angle of aperture. However, modelling the variation of such coupling, i.e., the change in the mutual inductance, with the angle of aperture does not seem to be an easy task with the considered geometry. Therefore, such mutual inductance can be considered to be angle dependent and a fitting parameter. Note that this applies also to the inductance L_c of the particle, since the current path varies with θ.

Figure 5(c) depicts the lumped element equivalent circuit model corresponding to a microstrip line loaded with a DB-DGS partially folded and oriented as shown in Fig. 5(a).

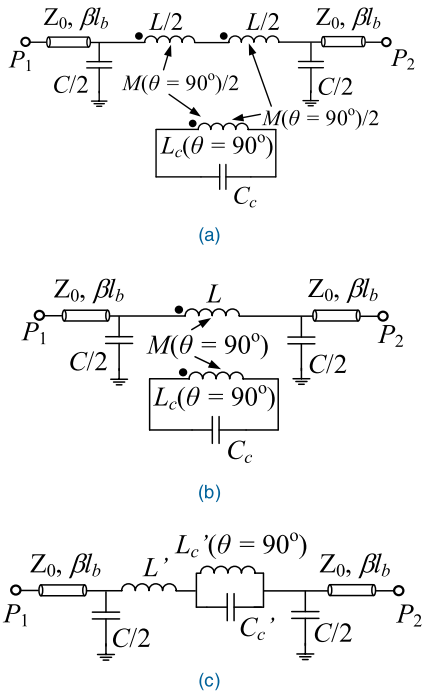

FIGURE 6. Circuit model of Fig. 5(c) for $\theta = 90°$ (a) transformed model with unification of the inductance and mutual coupling (b), and transformed circuit (c).

In the limit where $\theta = 0°$, the circuit of Fig. 5(c) transforms to the model of Fig. 4(b). By contrast, for an angle of aperture of $\theta = 90°$, corresponding to the topology of the unfolded DB-DGS resonator, the model of Fig. 5(c) should be the one of Fig. 2(b). It is apparent that for $\theta = 90°$, the coupling capacitance is null (i.e., $C(\theta = 90°) = 0$), whereas the capacitances of the extremes are simply $C/2$ (the line capacitance). The result is the π-model depicted in Fig. 6(a), where the resonant tank (i.e., the DB-DGS resonator) is excited exclusively by the mutual inductance M. This model can be transformed to the one of Fig. 6(b), and, finally, to the one of Fig. 6(c), where the equivalent inductance L' and the capacitances $C/2$, can be considered to describe the line section in the model of Fig. 2(b) corresponding to the length l. Therefore, the lumped element circuit model of Fig. 6(c) is equivalent to the one of Fig. 2(b). The element values of the series branch in the circuit of Fig. 6(c) can be derived by first obtaining the impedance of the series branch, i.e. [44],

$$Z_s = j\omega \cdot \left\{ L + \frac{M^2}{L_c(\frac{\omega_0^2}{\omega^2} - 1)} \right\} \tag{2}$$

Such impedance can be expressed as

$$Z_s = j\omega \cdot \left\{ L - L_c' + \frac{L_c'}{1 - L_c' C_c' \omega^2} \right\} \tag{3}$$

and it is apparent that this is the impedance of the series branch in the circuit of Fig. 6(c), with element values

given by

$$L' = L - L'_c \tag{4a}$$
$$L'_c = C_c M^2 \omega_0^2 \tag{4b}$$
$$C'_c = \frac{L_c}{M^2 \omega_0^2} \tag{4c}$$

and $\omega_0^2 = 1/L_c C_c = 1/L'_c C'_c$ (ω_0 is the angular frequency of the DB-DGS resonator).

In the previous analysis, it has been considered that the magnetic coupling between the apertures of the DB-DGS resonator can be neglected. This is reasonable as far as the distance between the apertures is significant, the case considered in this paper even for the folded DB-DGS (with $\theta = 0°$). Nevertheless, if the distance between the apertures is small and, consequently, inter-aperture coupling cannot be neglected, the effect is a modification of the equivalent inductance of the DB-DGS. The specific value is simply $L + M'/2$, where M' is the mutual coupling between the apertures.

The analysis has also neglected the effect of losses, since the main interest of the paper is to propose and validate a unified circuit model (the one of Fig. 5) able to predict the behavior of the DB-DGS-loaded microstrip line and the coupling mechanisms for any arbitrary angle of aperture, rather than to obtain an accurate circuit response. Moreover, in the specific structures used for validation, to be discussed next, losses are small, since low-loss microwave substrates (i.e., with low loss tangents) are considered, and ohmic losses, related to the metallic layers, are also small.

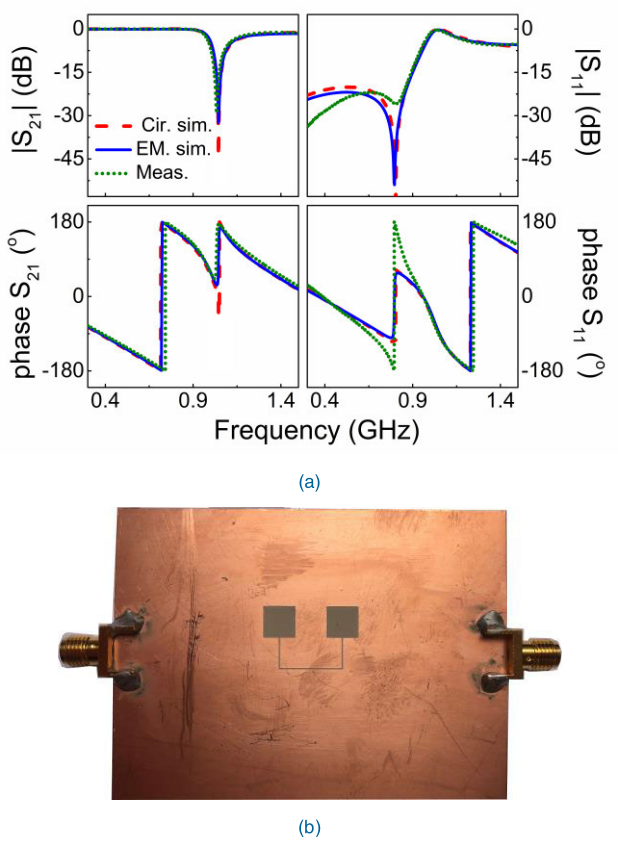

FIGURE 7. (a) Electromagnetic, circuit and measured responses of the structure of Fig. 3; (b) photograph of the fabricated structure (ground plane side).

III. MODEL VALIDATION

For model validation, the different DB-DGS and folded DB-DGS based microstrip lines (all exhibiting notched responses) are simulated by means of an electromagnetic solver (the *Keysight Momentum* commercial simulator). From such electromagnetic simulations, the circuit parameters are extracted and used to obtain the circuit responses, which are compared to the full-wave electromagnetic simulations. The considered substrate is the *Rogers RO3010* with dielectric constant $\varepsilon_r = 10.2$ and thickness $h = 1.27$ mm. In such substrate the width of a 50-Ω line is found to be $W = 1.1$ mm, the considered value. Concerning the dimensions of the DB-DGS, the apertures are square shaped and exhibit a side length of $l/2$, whereas the total length of the narrow slot is $2l$, with $l = 12$ mm. The width of the slot is 0.2 mm. For the folded DB-DGS with $\theta = 0°$, the distance between the apertures is also $l/2$, and such distance progressively increases as the angle of aperture increases (see Fig. 3(a) for details).

The first structure under consideration is the microstrip line loaded with the folded DB-DGS oriented as depicted in Fig. 3(a), since this structure exhibits exclusively electric coupling and the circuit model is, thus, relatively simple, see Fig. 3(b). Moreover, parameter extraction with such circuit model has been reported in the literature [45]. The electromagnetic response of this structure is depicted in Fig. 7(a). The extracted parameters, inferred by means of the method of [45], are: $L = 9.27$ nH, $C = 2.07$ pF, $L_c = 3.69$ nH, and $C_c = 4.23$ pF. The circuit response, also included in the figure, is in good agreement with the electromagnetic simulation, which indicates that the model provides an accurate description of the structure. Such structure has been fabricated by means of the *LPKF-H100* drilling machine, available in the laboratory of the research group [Fig. 7(b)]. The measured response, depicted in Fig. 7(a), is also in good agreement with the circuit and electromagnetic responses The small discrepancies are mainly due to the effects of losses, and to fabrication related tolerances (radiation losses are small, as inferred from the simulated loss factor, not shown, calculated by excluding ohmic an dielectric losses). It should be clarified that for parameter extraction, the effects of the 50-Ω access lines, with length l_b, have been omitted, but then, in the simulations, such lines have been included. In the measurements, the port extension function of the vector network analyzer (VNA) has been used to correct the phase shift introduced by the connectors.

Next, the electromagnetic response of the structure that results from the structure of Fig. 3 by rotating the folded DB-DGS 90° has been inferred [Fig. 4(a)]. The hypothesis that such rotation in the orientation of the resonator does not modify the circuit parameters of the line (including the

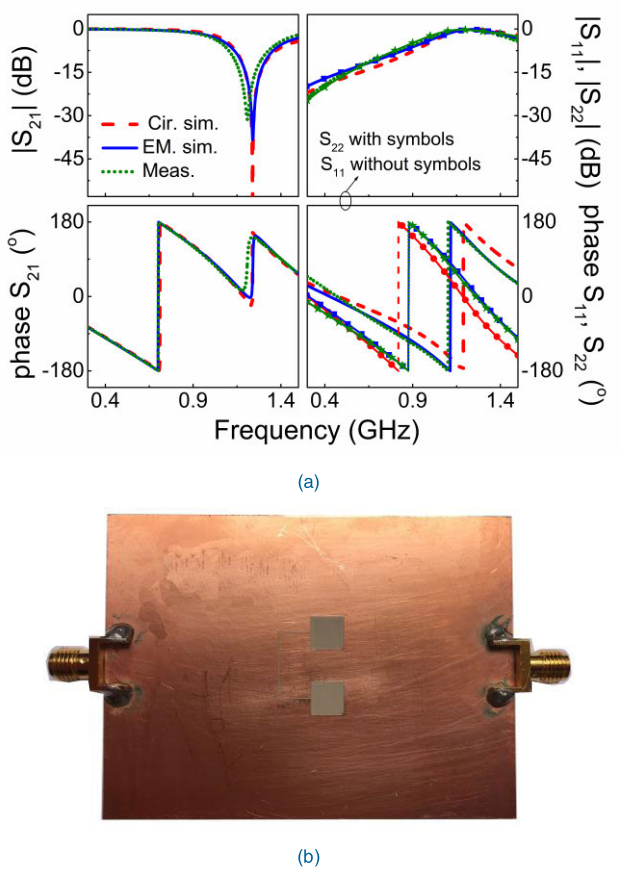

FIGURE 8. (a) Electromagnetic, circuit and measured responses of the structure of Fig. 4; (b) photograph of the fabricated structure (ground plane side). S_{11} and S_{22} magnitude for both EM simulation and circuit simulation are nearly undistinguishable.

coupling capacitance) and the capacitance of the resonator, has been made, as anticipated before. However, the inductance of the resonator, L_c, is considered to be an adjustable parameter, as far as it is expected to change by rotating the DB-DGS resonator, as justified in the preceding section. Thus, the inductance L_c and the mutual inductance M have been inferred by curve fitting, and the resulting values have been found to be: $L_c = 2.80$ nH and $M = 2.86$ nH. Figure 8(a) depicts the circuit, electromagnetic and measured responses, where the agreement is, again, very reasonable (the slight frequency shift in the measured resonant frequency is due to fabrication related tolerances). Note that, due to the lack of symmetry with regard to the bisecting plane between the input and the output ports, the S-parameter matrix is not symmetric, i.e., $S_{11} \neq S_{22}$.

The next step has been to consider the structure of Fig. 2, with completely unfolded ($\theta = 90°$) and transversally oriented DB-DGS resonator. The same hypothesis assumed before is adopted here, i.e., L, C, and C_c are not altered by unfolding the resonator. Thus, again, L_c and M are fitting parameters. The values providing the best agreement between the electromagnetic simulation and circuit response, see Fig. 9(a), have been found to be $L_c(\theta = 90°) = 3.51$ nH and $M(\theta = 90°) = 4.0$ nH. Since the electric coupling in this configuration vanishes (the DB-DGS is excited exclusively by means of the magnetic field generated by the line), the circuit is symmetric with regard to the bisecting plane between the input and output ports, in agreement with the topology of the structure, also symmetric with regard to that plane. Thus, in this case, it follows that matching is identical from both ports (i.e., $S_{11} = S_{22}$). The measured response, also included in Fig. 9(a), is in reasonably good agreement with the simulated and circuit responses (the origin of the small discrepancies has been indicated in reference to the previous results).

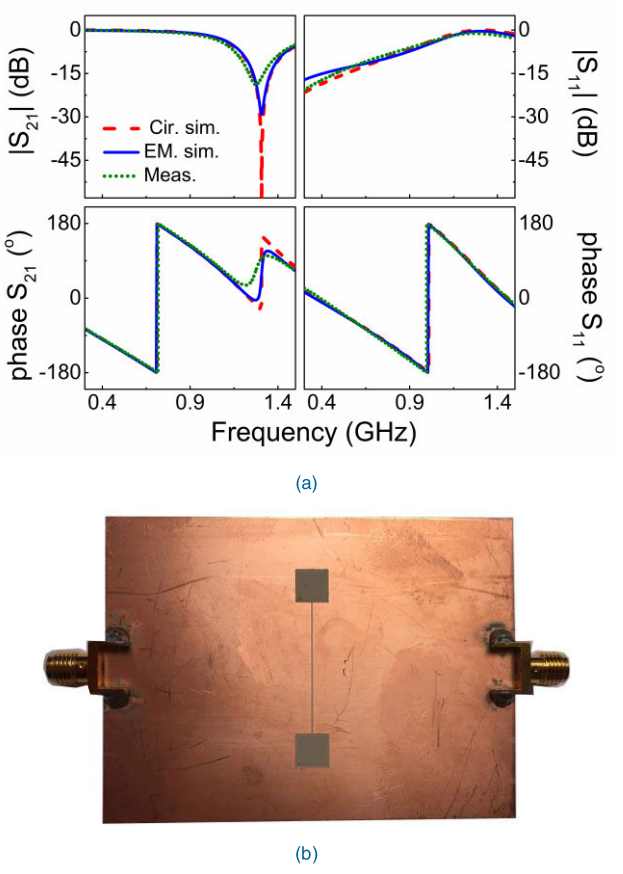

FIGURE 9. (a) Electromagnetic, circuit and measured responses of the structure of Fig. 2; (b) photograph of the fabricated structure (ground plane side).

Finally, we have considered a partially folded DB-DGS resonator with folding level given by $\theta = 45°$. According to the model, see Fig. 5, the line inductance, L, is preserved, as compared to the previous cases, whereas the line capacitance corresponding to the length l is divided in three parts, all dependent on the folding angle θ. Nevertheless, it is assumed that the contribution of the three capacitances, C, does not vary in comparison to the previous cases. According to (1), the capacitance portion coupled to the resonant element is $C(\theta = 45°) = 1.46$ pF, whereas the capacitances of the extremes are $[C - C(\theta = 45°)]/2 = 0.30$ pF. It is also assumed that the capacitance of the resonator C_c does not vary. Thus,

the fitting parameters are, again, L_c and M, and the values that have provided the best fitting have been found to be $L_c(\theta = 45°) = 2.85$ nH and $M(\theta = 45°) = 3.36$ nH. Figure 10(a) depicts the simulated, circuit, and measured responses for $\theta = 45°$. Naturally, in this case, $S_{11} \neq S_{22}$, as expected on account of the lack of symmetry due to partial folding. In the circuit model, the mixed coupling destroys the symmetry, similar to the case of Figs. 4 and 8.

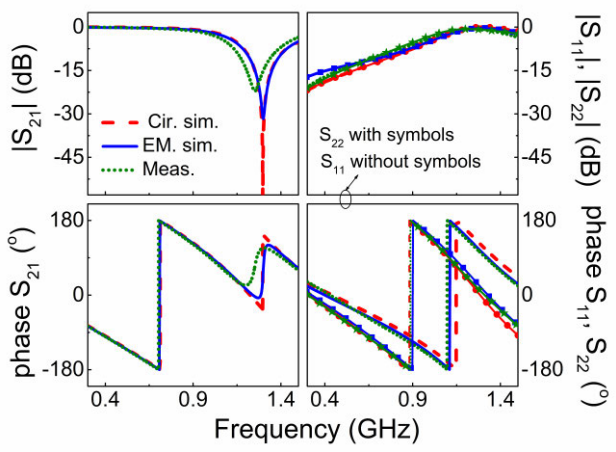

(a)

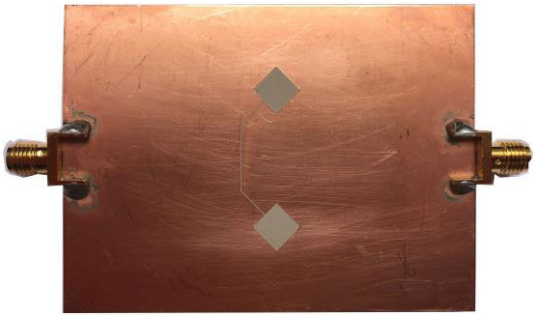

(b)

FIGURE 10. (a) Electromagnetic, circuit and measured responses of the structure of Fig. 5 and $\theta = 45°$; (b) photograph of the fabricated structure (ground plane side).

According to the results presented in Fig. 10(a), the agreement between the circuit, electromagnetic and measured responses is also reasonable. These results validate the proposed model of Fig. 5, where the capacitance of the line section l is divided in three different portions, which depend on the angle of aperture of the DB-DGS resonator. Nevertheless, the total capacitance C neither depends on the angle of aperture of the resonator, nor on the angle of orientation of the DB-DGS resonator.

IV. DISCUSSION

To gain more insight on the dependence of $C(\theta)$, $L_c(\theta)$, and $M(\theta)$ with the folding (aperture) angle, we have simulated (but not fabricated) additional DB-DGS-loaded microstrip lines with different angles of aperture of the folded resonator. The parameters, inferred by curve fitting, are summarized in Table 1 (the simulations are not shown). Note that $C(\theta)$, rather than fitted, it has been calculated by means of expression (1), taking into account that $C(\theta = 0°) = 2.07$ pF. The table includes also the coupling coefficient, k, between the line inductance and the inductance of the DB-DGS resonator, defined as $k = M/\sqrt{LL_c}$.

TABLE 1. Dependence of model parameters with the angle θ.

θ	$C(\theta)$ (pF)	$L_c(\theta)$ (nH)	$M(\theta)$ (nH)	k
0°	2.07	2.79	2.86	0.56
15°	2.00	2.71	3.00	0.60
30°	1.79	2.76	3.20	0.63
45°	1.46	2.85	3.36	0.65
60°	1.03	3.02	3.60	0.68
75°	0.53	3.26	3.84	0.70
90°	0	3.50	4.00	0.70

According to the results of Table 1, the inductance of the resonant element, L_c, does not appreciably change for angles of aperture below 45°, and it increases with θ when $\theta > 45°$. By contrast, M experiences a progressive growth with θ for angles between $0° < \theta < 90°$. However, the coupling coefficient, k, does not significantly vary with θ. It slightly increases with the angle of aperture of the DB-DGS, but it tends to saturate as θ approaches 90°. This behavior is attributed to the fact that, for angles of aperture close to 90°, the magnetic field generated by the line impacts only the narrow slot region of the DGS in the vicinity of the line strip. Consequently, the coupling coefficient should not significantly vary with θ for apertures close to 90°. By contrast, for small aperture angles, the regions of the folded DB-DGS under the influence of the magnetic field generated by the line are not restricted to the narrow slot region beneath the line. The square-shaped apertures may interact with the line, but such interaction is expected to decrease with θ. It is believed that the increase of L_c with the aperture angle is related to the progressively decreasing influence of the strip line on this parameter, as such angle increases (i.e., by increasing the angle, the influence of the line is less severe). This increase in L_c is thought to be the reason of an increase in M, provided k, the coupling coefficient, is roughly constant. Nevertheless, an exact calculation of the coupling coefficient and an accurate explanation of the involved phenomenology is complex, since the geometry of the considered folded DB-DGS is not simple.

Let us analyze in more detail the line loaded with the unfolded and transversally oriented DB-DGS resonator. Using expressions (4), the parameters of the transformed model of Fig. 6(c) are found to be $L' = 4.72$ nH, $L'_c = 4.55$ nH and $C'_c = 3.26$ pF. Obviously, the capacitances $C/2$ of the shunt branches of the model of Fig. 6 are not affected by the transformation. Let us now directly infer the parameters of the circuit model of Fig. 6(c), excluding C, by parameter extraction from the electromagnetically simulated response (see Fig. 9(a)). The results are, $L' = 5.46$ nH, $L'_c = 4.37$ nH

and $C_c' = 3.40$ pF i.e., in reasonably good agreement with the parameters of the series branch obtained by means of expressions (4). Figure 11 compares the circuit responses inferred by considering both sets of parameters. The figure includes also the EM simulation of the structure (also depicted in Fig. 9(a)). The agreement between the three responses is good.

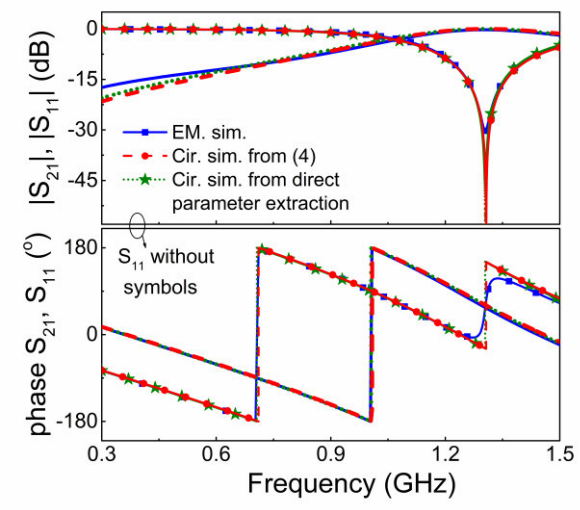

FIGURE 11. Comparison between the circuit response of the structure of Fig. 9(a), given by the model of Fig. 6(c), obtained by the two sets of reactive parameters indicated in the text, i.e., from the transformation equations (4) and from direct parameter extraction. The electromagnetically simulated response is also included.

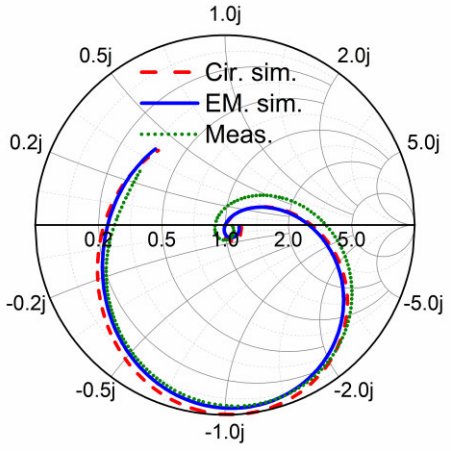

FIGURE 12. Detail of S_{11} corresponding to the structure of Fig. 7, represented in the Smith Chart.

There is a difference between the model of Fig. 2(b) and the model of Fig. 6(c), namely, the presence of L' and C in the latter. Because the general lumped element model of Figure 5 accounts for the DB-DGS plus the line section of length l, the model of Fig. 6 should include such line section, and, indeed, L' and C model such line section. By contrast, in the model of Fig. 2, the usual model of a microstrip line loaded with an unfolded and transversally oriented DB-DGS resonator, the lumped elements are restricted to the description of the resonant element. Note that in the model of Fig. 2(b), the line sections account for the whole line, whereas in the model of Fig. 6(c), the line sections describe only the access lines by excluding the central part of length l. Thus, according to these words, the values of L' and C in the circuit of Fig. 6(c) should be coherent with the inductance and capacitance of the 50-Ω line corresponding to the considered line length l. Indeed, such coherence is verified as far as the characteristic impedance given by these reactive parameters, i.e., $\sqrt{L'/C}$, coincides to a very good approximation with the nominal characteristic impedance of the line (50 Ω). Particularly, by considering L' inferred from the transformations (4), i.e., $L' = 4.72$ nH, one obtains $\sqrt{L'/C} = 47.8$ Ω, whereas with $L' = 5.46$ nH (extracted value), the characteristic impedance is found to be $\sqrt{L'/C} = 51.4$ Ω. In both cases, $C = 2.07$ pF. On the other hand, the electrical length of the line section l is $\beta l = \omega\sqrt{L'C}$. At the resonance frequency of the DB-DGS resonator, $f_0 = 1.305$ GHz, the electrical length is found to be $\beta l = 0.81$ rad for $L' = 4.72$ nH, and $\beta l = 0.87$ rad for $L' = 5.46$ nH. These phases are in reasonable agreement with the nominal electrical length of the line section of length l, inferred from the transmission line calculator *LineCalc* (included in *Keysight ADS*) using the parameters of the considered substrate (0.87 rad). Consequently, it can be concluded that L' and C in the model of Fig. 6(c) describe the line section of length l, whereas the access lines of length l_b are accounted for by the corresponding transmission line sections. In the model of Fig. 2(b), the access lines of length l_a describe the complete line strip. Nevertheless, it is clear according to this discussion that the models of Figs. 2(b) and 6(c) are equivalent.

Another interesting aspect to discuss is the discrepancy in the phase response of S_{11} (between circuit/electromagnetic simulation and measurement) for the structure of Fig. 7 (the difference in magnitude has been attributed to the effects of losses, and due to the fact that losses preclude from obtaining a "true" reflection zero). The difference in the phase of S_{11} is more subtle, and further insight can be inferred from the representation of S_{11} in the Smith Chart, as shown in Fig. 12. At the reflection zero frequency, when losses are negligible, there is a cross through the center of the Smith Chart (with, theoretically, total transmission), and therefore the phase changes suddenly (jumps) from roughly $-90°$ to $+90°$, corresponding approximately to a vertical cross through the center of the Smith Chart. However, in measurement, due to the effect of losses, the trace of S_{11} crosses the horizontal axis of the Smit Chart (where the impedance is purely resistive) slightly to the left of the center, and therefore the phase jump is exactly from $-180°$ to $+180°$. So, this higher (360°) jump in measurement is explained by this fact. Therefore, this apparent high discrepancy in S_{11} between measurement and simulated values is in reality an artifact (as it can be appreciated in the Smith Chart, the difference between measurements and simulations is not very significant).

To end this section let us mention that if a gap capacitor is etched in the strip line, aligned with the narrow slot of the transversally oriented folded, or partially folded, DB-DGS resonator, then it is expected that the notched response switches to a bandpass response. However, the corresponding modelling is out of the scope of this paper. Let us also emphasize that the considered lossless circuit models predict the behavior of the considered structures to a good approximation, since the considered substrate exhibits small losses. This good agreement would also be expected by considering other low-loss microwave substrates such as those of the *Rogers RO3006* and *RO4003C* series.

V. CONCLUSION

In this paper, the modelling of a microstrip transmission line loaded with a DB-DGS resonator with an arbitrary angle of aperture, and oriented with its symmetry plane aligned with the line axis, or rotated 90°, has been studied. It has been shown that when the symmetry plane of the DB-DGS is orthogonal to the line axis, the coupling between the line and the resonator is exclusively electric. By contrast, when the symmetry plane of the DB-DGS is aligned with the axis of the line, the driving mechanism of the resonant element includes electric and magnetic coupling (mixed coupling), unless the DB-DGS resonator is unfolded. In this later case, electric coupling vanishes, and the coupling mechanism is purely magnetic. A circuit model that takes into account the folding level of the resonator, quantified by the angle of aperture θ, has been proposed for the first time. With the results of this work, it is clear that such angle dependent model (depicted in Fig. 5), with mixed coupling, is able to describe the behavior of the folded and unfolded DB-DGS with transverse orientation, regardless of the aperture angle θ. Moreover, it has been shown that the model is compatible with the commonly accepted model of the unfolded DB-DGS, consisting of a parallel resonant tank series-connected to the line. In this case, the coupling between the line and the resonator is exclusively magnetic, as indicated above. By contrast, for the folded or partially folded DB-DGS resonator, mixed coupling (magnetic and electric) should be considered, and electric coupling is a maximum when the angle of aperture is $\theta = 0°$ (completely folded resonator). However, by rotating the folded resonator 90° with regard to the line, magnetic coupling vanishes, and the particle is driven only by the electric field generated by the line. Arbitrary angular orientations between the line and the resonator have not been considered, but it is obvious that the effect of such rotation is a modulation of the magnetic coupling between the line and the DB-DGS resonator. Nevertheless, modeling this angle dependent mutual coupling is complex with the considered resonator topology, and this aspect has not been considered in this paper. Microwave engineers to date have exhaustively used the DB-DGS resonator, but a study of the type pointed out in this paper has never been carried out before. The results of this paper may thus be worthy for many researchers working in circuit modelling, planar filters, and planar microwave sensors.

REFERENCES

[1] C. S. Kim, J. S. Park, D. Ahn, and J. B. Lim, "A novel 1-D periodic defected ground structure for planar circuits," *IEEE Microw. Wireless Lett.*, vol. 10, no. 4, pp. 131–133, Apr. 2000.
[2] L. H. Weng, Y.-C. Guo, X.-W. Shi, and X.-Q. Chen, "An overview on defected ground structure," *Prog. Electromagn. Res. B*, vol. 7, pp. 173–189, Apr. 2008.
[3] M. K. Khandelwal, B. K. Kanaujia, and S. Kumar, "Defected ground structure: Fundamentals, analysis, and applications in modern wireless trends," *Int. J. Antennas Propag.*, vol. 2017, Feb. 2017, Art. no. 2018527.
[4] J.-X. Chen, J. Shi, Z.-H. Bao, and Q. Xue, "Tunable and switchable bandpass filters using slot-line resonators," *Prog. Electromagn. Res.*, vol. 111, pp. 25–41, Nov. 2010.
[5] F. Falcone, T. Lopetegi, J. D. Baena, R. Marqués, F. Martín, and M. Sorolla, "Effective negative-stop-band microstrip lines based on complementary split ring resonators," *IEEE Microw. Wireless Compon. Lett.*, vol. 14, no. 6, pp. 280–282, Jun. 2004.
[6] J. Selga, G. Sisó, M. Gil, J. Bonache, and F. Martín, "Microwave circuit miniaturization with complementary spiral resonators: Application to high-pass filters and dual-band components," *Microw. Opt. Technol. Lett.*, vol. 51, no. 11, pp. 2741–2745, Nov. 2009.
[7] O. Isik, K. P. Esselle, and Y. Ge, "Harmonic control of active microstrip antennas using spiral defected ground structures," in *Proc. 10th Austral. Symp. Antennas*, Sydney, NSW, Australia, Feb. 2007, pp. 14–15.
[8] A. K. Horestani, M. Durán-Sindreu, J. Naqui, C. Fumeaux, and F. Martín, "S-shaped complementary split ring resonators and their application to compact differential bandpass filters with common-mode suppression," *IEEE Microw. Wireless Compon. Lett.*, vol. 24, no. 3, pp. 150–152, Mar. 2014.
[9] J. Naqui, M. Durán-Sindreu, and F. Martín, "Differential and single-ended microstrip lines loaded with slotted magnetic-LC resonators," *Int. J. Antennas Propag.*, vol. 2013, Jun. 2013, Art. no. 640514.
[10] A. Ebrahimi, T. C. Baum, K. Wang, J. Scott, and K. Ghorbani, "Differential transmission lines loaded with magnetic LC resonators and application in common mode suppression," *IEEE Trans. Circuits Syst.*, vol. 66, no. 10, pp. 3811–3821, Oct. 2019.
[11] D. Ahn, J. S. Park, C. S. Kim, J. Kim, Y. Qian, and T. Itoh, "A design of the low-pass filter using the novel microstrip defected ground structure," *IEEE Trans. Microw. Theory Techn.*, vol. 49, no. 1, pp. 86–93, Jan. 2001.
[12] J. Bonache, F. Martín, J. García-García, I. Gil, R. Marqués, and M. Sorolla, "Ultra wide band pass filters (UWBPF) based on complementary split rings resonators," *Microw. Opt. Technol. Lett.*, vol. 46, no. 3, pp. 283–286, Aug. 2005.
[13] A. M. E. Safwat, F. Podevin, P. Ferrari, and A. Vilcot, "Tunable bandstop defected ground structure resonator using reconfigurable dumbbell-shaped coplanar waveguide," *IEEE Trans. Microw. Theory Techn.*, vol. 54, no. 9, pp. 3559–3564, Sep. 2006.
[14] J. Bonache, I. Gil, J. García-García, and F. Martín, "Novel microstrip bandpass filters based on complementary split-ring resonators," *IEEE Trans. Microw. Theory Techn.*, vol. 54, no. 1, pp. 265–271, Jan. 2006.
[15] M. K. Mandal and S. Sanyal, "A novel defected ground structure for planar circuits," *IEEE Microw. Wireless Compon. Lett.*, vol. 16, no. 2, pp. 93–95, Feb. 2006.
[16] Z.-Z. Hou, "Novel wideband filter with a transmission zero based on split-ring resonator DGS," *Microw. Opt. Technol. Lett.*, vol. 50, no. 6, pp. 1691–1693, 2008.
[17] S. N. Burokur, M. Latrach, and S. Toutain, "A novel type of microstrip coupler utilizing a slot split-ring resonators defected ground plane," *Microw. Opt. Technol. Lett.*, vol. 48, no. 1, pp. 138–141, Jan. 2006.
[18] J. Bonache, G. Siso, M. Gil, Á. Iniesta, J. Garcia-Rincon, and F. Martin, "Application of composite right/left handed (CRLH) transmission lines based on complementary split ring resonators (CSRRs) to the design of dual-band microwave components," *IEEE Microw. Wireless Compon. Lett.*, vol. 18, no. 8, pp. 524–526, Aug. 2008.
[19] A. Ebrahimi, T. Baum, and K. Ghorbani, "Differential bandpass filters based on dumbbell-shaped defected ground resonators," *IEEE Microw. Wireless Compon. Lett.*, vol. 28, no. 2, pp. 129–131, Feb. 2018.

[20] S. U. Rehman, A. F. Sheta, and M. Alkanhal, "Compact bandstop filter using defected ground structure (DGS)," in *Proc. Saudi Int. Electron., Commun. Photon. Conf. (SIECPC)*, Riyadh, Saudi Arabia, Apr. 2011, pp. 1–4, doi: 10.1109/SIECPC.2011.5876972.
[21] A. Abdel-Rahman, A. R. Ali, S. Amari, and A. S. Omar, "Compact bandpass filters using defected ground structure (DGS) coupled resonators," in *IEEE MTT-S Int. Microw. Symp. Dig.*, Long Beach, CA, USA, Jun. 2005, pp. 1479–1482.
[22] S. U. Rehman, A. F. Sheta, and M. A. Alkanhal, "Compact bandpass filters with bandwidth control using defected ground structure (DGS)," *Appl. Comput. Electromagn. Soc. J.*, vol. 26, no. 7, pp. 624–630, Jul. 2011.
[23] Z. Zeng, S. J. Chen, and C. Fumeaux, "A reconfigurable filter using defected ground structure for wideband common-mode suppression," *IEEE Access*, vol. 7, pp. 36980–36990, 2019.
[24] M. Esa, U. Jamaluddin, and M. S. Awang, "Antenna with DGS for improved performance," in *Proc. IEEE Asia–Pacific Conf. Appl. Electromagn. (APACE)*, Port Dickson, Malaysia, Nov. 2010, doi: 10.1109/APACE.2010.5719754.
[25] R. K. Yadav, S. Das, and R. L. Yadava, "DGS based microstrip patch antennas for UWB systems," in *Proc. 3rd IEEE Int. Advance Comput. Conf. (IACC)*, Ghaziabad, India, Feb. 2013, pp. 1573–1576.
[26] F. A. L. B. Konkyana and B. A. Sudhakar, "A review on microstrip antennas with defected ground structure techniques for ultra-wideband applications," in *Proc. Int. Conf. Commun. Signal Process. (ICCSP)*, Chennai, India, Apr. 2019, pp. 930–934.
[27] D. Gopi, A. R. Vadaboyina, and J. R. K. K. Dabbakuti, "DGS based monopole circular-shaped patch antenna for UWB applications," *Social Netw. Appl. Sci.*, vol. 3, no. 2, p. 198, Feb. 2021.
[28] A. Ebrahimi, W. Withayachumnankul, S. Al-Sarawi, and D. Abbott, "High-sensitivity metamaterial-inspired sensor for microfluidic dielectric characterization," *IEEE Sensors J.*, vol. 14, no. 5, pp. 1345–1351, May 2014.
[29] A. Ebrahimi, W. Withayachumnankul, S. F. Al-Sarawi, and D. Abbott, "Dual-mode behavior of the complementary electric-LC resonators loaded on transmission line: Analysis and applications," *J. Appl. Phys.*, vol. 116, no. 8, Aug. 2014, Art. no. 083705.
[30] L. Su, J. Mata-Contreras, P. Vélez, and F. Martín, "Splitter/combiner microstrip sections loaded with pairs of complementary split ring resonators (CSRRs): Modeling and optimization for differential sensing applications," *IEEE Trans. Microw. Theory Techn.*, vol. 64, no. 12, pp. 4362–4370, Dec. 2016.
[31] L. Su, J. Mata-Contreras, P. Vélez, A. Fernández-Prieto, and F. Martín, "Analytical method to estimate the complex permittivity of oil Samples," *Sensors*, vol. 18, no. 4, p. 984, 2018.
[32] P. Velez, K. Grenier, J. Mata-Contreras, D. Dubuc, and F. Martin, "Highly-sensitive microwave sensors based on open complementary split ring resonators (OCSRRs) for dielectric characterization and solute concentration measurement in liquids," *IEEE Access*, vol. 6, pp. 48324–48338, 2018.
[33] J. Yeo and J.-I. Lee, "High-sensitivity microwave sensor based on an interdigital-capacitor-shaped defected ground structure for permittivity characterization," *Sensors*, vol. 19, no. 3, p. 498, Jan. 2019.
[34] P. Vélez, J. Muñoz-Enano, M. Gil, J. Mata-Contreras, and F. Martín, "Differential microfluidic sensors based on dumbbell-shaped defect ground structures in microstrip technology: Analysis, optimization, and applications," *Sensors*, vol. 19, no. 14, p. 3189, Jul. 2019.
[35] J. Munoz-Enano, P. Velez, C. Herrojo, M. Gil, and F. Martin, "On the sensitivity of microwave sensors based on slot resonators and frequency variation," in *Proc. Int. Conf. Electromagn. Adv. Appl. (ICEAA)*, Granada, Spain, Sep. 2019, pp. 0112–0115.
[36] J. Muñoz-Enano, P. Vélez, M. Gil, E. Jose-Cunilleras, A. Bassols, and F. Martín, "Characterization of electrolyte content in urine samples through a differential microfluidic sensor based on dumbbell-shaped defected ground structures," *Int. J. Microw. Wireless Technol.*, vol. 12, no. 9, pp. 817–824, Nov. 2020.
[37] J. Muñoz-Enano, P. Vélez, M. Gil, and F. Martín, "Planar microwave resonant sensors: A review and recent developments," *Appl. Sci.*, vol. 10, no. 7, p. 2615, 2020.
[38] M. Makimoto and S. Yamashita, "Compact bandpass filters using stepped impedance resonators," *Proc. IEEE*, vol. 67, no. 1, pp. 16–19, Jan. 1979.
[39] J. Naqui, M. Durán-Sindreu, J. Bonache, and F. Martín, "Implementation of shunt connected series resonators through stepped-impedance shunt stubs: Analysis and limitations," *IET Microw., Antennas Propag.*, vol. 5, pp. 1336–1342, Aug. 2011.
[40] W.-T. Liu, C.-H. Tsai, T.-W. Han, and T.-L. Wu, "An embedded common-mode suppression filter for GHz differential signals using periodic defected ground plane," *IEEE Microw. Wireless Compon. Lett.*, vol. 18, no. 4, pp. 248–250, Apr. 2008.
[41] J. S. Hong and M. J. Lancaster, *Microstrip Filters for RF/Microwave Applications*. Hoboken, NJ, USA: Wiley, 2001.
[42] D.-J. Woo and T.-K. Lee, "An equivalent circuit model for a dumbbell-shaped DGS microstrip line," *J. Electromagn. Eng. Sci.*, vol. 14, no. 4, pp. 415–418, Dec. 2014.
[43] J. Naqui, M. Duran-Sindreu, and F. Martin, "Modeling split-ring resonator (SRR) and complementary split-ring resonator (CSRR) loaded transmission lines exhibiting cross-polarization effects," *IEEE Antennas Wireless Propag. Lett.*, vol. 12, pp. 178–181, 2013.
[44] F. Martin, *Artificial Transmission Lines for RF and Microwave Applications*. Hoboken, NJ, USA: Wiley, 2015.
[45] J. Bonache, M. Gil, I. Gil, J. García-García, and F. Martín, "On the electrical characteristics of complementary metamaterial resonators," *IEEE Microw. Wireless Compon. Lett.*, vol. 16, no. 10, pp. 543–545, Oct. 2006.

LIJUAN SU (Member, IEEE) was born in Qianjiang, Hubei, China, in 1983. She received the B.S. degree in communication engineering and the M.S. degree in circuits and systems from the Wuhan University of Technology, Wuhan, China, in 2005 and 2013, respectively, and the Ph.D. degree in electronic engineering from the Universitat Autonoma de Barcelona, Barcelona, Spain, in 2017. From November 2017 to December 2019, she worked as a Postdoctoral Researcher with the Flexible Electronics Research Center, Huazhong University of Science and Technology, Wuhan. She is currently a Postdoctoral Researcher under the support of the Juan de la Cierva Program with the CIMITEC, Universitat Autonoma de Barcelona. Her current research interests include development of novel microwave sensors with improved performance for biosensors, dielectric characterization of solids and liquids, defect detection, and industrial processes.

JONATHAN MUÑOZ-ENANO (Member, IEEE) was born in Mollet del Vallès, Barcelona, Spain, in 1994. He received the bachelor's degree in electronic telecommunications engineering and the master's degree in telecommunications engineering from the Universitat Autonoma de Barcelona (UAB), in 2016 and 2018, respectively, where he is currently pursuing the Ph.D. degree, which is focused on the development of microwave sensors based on metamaterials concepts for the dielectric characterization of materials and biosensors.

PARIS VÉLEZ (Senior Member, IEEE) was born in Barcelona, Spain, in 1982. He received the degree in telecommunications engineering, specializing in electronics, and the Electronics Engineering degree and the Ph.D. degree in electrical engineering from the Universitat Autònoma de Barcelona, Barcelona, in 2008, 2010, and 2014, respectively. His Ph.D. thesis concerned common mode suppression differential microwave circuits based on metamaterial concepts and semi-lumped resonators. During his Ph.D., he was awarded with a pre-doctoral teaching and research fellowship by the Spanish Government, from 2011 to 2014. From 2015 to 2017, he was involved in the subjects related to metamaterials sensors for fluidics detection and characterization at LAAS-CNRS through a TECNIOSpring fellowship, co-founded by the Marie Curie Program. His current research interests include the miniaturization of passive circuits RF/microwave and sensors-based metamaterials through Juan de la Cierva Fellowship. He is a Reviewer of the IEEE TRANSACTIONS ON MICROWAVE THEORY AND TECHNIQUES and for other journals.

JESÚS MARTEL (Senior Member, IEEE) received the Licenciado and Ph.D. degrees in physics from the University of Seville, Seville, Spain, in 1989 and 1996, respectively. Since 1990, he has performed research with the Microwave Group, University of Seville. He is currently a Professor with the Department of Applied Physics II, University of Seville, where he was the Head of the Department, from 2010 to 2018. His current research interests include the numerical analysis of planar transmission lines, the modeling of planar microstrip discontinuities, the design of passive microwave circuits, the techniques in microwave measurements, and the proprieties of artificial media.

FRANCISCO MEDINA (Fellow, IEEE) was born in Puerto Real, Cádiz, Spain, in 1960. He received the Licenciado (5-year) degree *(summa cum laude)* in physics (electronics) and the Ph.D. degree *(cum laude)* in physics (microwaves) from the University of Seville, Seville, Spain, in 1983 and 1987, respectively.

Afterwards, he spent one year with the group headed by Prof. Henri Baudrand at ENSEEIHT, Toulouse, France, as a Postdoctoral Researcher thanks to another competitive fellowship granted by the Spanish and French governments. Then he joined as an Assistant Professor, the group headed by Prof. Manuel Horno at the Department of Electronics and Electromagnetism, Physics Faculty, University of Seville, in 1987, where he became an Associate Professor, in 1990, and then a Full Professor, in 2009. Since 1998, he has been the Head of the Microwave Group, University of Seville. During the last 38 years, he has been working on several topics related to applied electromagnetism and microwave engineering, including the modeling of planar transmission lines, antennas and circuits using optimized integral equation methods, (bi)anisotropic structures, metamaterials, and periodic electromagnetic structures. He has also contributed to the design of a variety of novel planar passive devices. This research has mainly been reported in a co-edited book *Balanced Microwave Filters* (John Wiley & Sons Inc. and IEEE-Press 2018), a dozen book chapters, more than 165 JCR journal articles and more than 340 conference contributions.

Dr. Medina was a recipient of a Research Fellowship of the Spanish Government during his Ph.D. training period. He was a recipient of a Salvador de Madariaga Fellowship during a four months visiting scholar stay with Prof. Yang Hao at QMUL, London, U.K. A few of these conference or journal contributions have received "best paper awards," including the recently awarded 2020 *IEEE Microwave Magazine* Best Paper Award. He is also the Editor-in-Chief of *International Journal of Microwave and Wireless Technologies*. He has also been a reviewer for more than 75 different journals, mainly in the fields of microwave and antenna engineering, optics, and applied physics. He has also co-organized the 2017 IEEE-MTT NEMO Symposium, Seville, Spain, and collaborates as a TPC member or a reviewer with a number of major conferences in the fields of microwave engineering, antenna engineering, and electromagnetic theory. Since 2017, he has been the President of the Spanish URSI Committee.

FERRAN MARTÍN (Fellow, IEEE) was born in Barakaldo, Vizcaya, Spain, in 1965. He received the B.S. degree in physics from the Universitat Autònoma de Barcelona (UAB), in 1988, and the Ph.D. degree, in 1992.

From 1994 to 2006, he was an Associate Professor of electronics with the Departament d'Enginyeria Electrònica, UAB. Since 2007, he has been a Full Professor of electronics. In recent years, he has been involved in different research activities, including modeling and simulation of electron devices for high frequency applications, millimeter wave and THz generation systems, and the application of electromagnetic bandgaps to microwave and millimeter wave circuits. He is very active in the field of metamaterials and their application to the miniaturization and optimization of microwave circuits and antennas. Other topics of interests include microwave sensors and RFID systems, with special emphasis on the development of high data capacity chipless-RFID tags. He is currently the Head of the Microwave Engineering, Metamaterials and Antennas Group (GEMMA Group), UAB, and the Director of CIMITEC, a Research Center on Metamaterials supported by TECNIO (Generalitat de Catalunya). He has organized several international events related to metamaterials and related topics, including Workshops at the IEEE International Microwave Symposium (2005 and 2007) and the European Microwave Conference (2009, 2015, and 2017), and the Fifth International Congress on Advanced Electromagnetic Materials in Microwaves and Optics (Metamaterials 2011), where he acted as the Chair of the Local Organizing Committee. He has authored or coauthored over 650 technical conference papers, letter, journal articles, and book chapters. He is the coauthor of the book on Metamaterials entitled *Metamaterials with Negative Parameters: Theory, Design and Microwave Applications* (John Wiley & Sons Inc.), an author of the book *Artificial Transmission Lines for RF and Microwave Applications* (John Wiley & Sons Inc.), a co-editor of the book *Balanced Microwave Filters* (Wiley/IEEE Press), and a coauthor of the book *Time-Domain Signature Barcodes for Chipless-RFID and Sensing Applications* (Springer). He has generated 21 Ph.D., has filed several patents on metamaterials, and has headed several Development Contracts. He has acted as a guest editor for six special issues on metamaterials and sensors in five international journals. He is a fellow of the IET. He is a member of the IEEE Microwave Theory and Techniques Society (IEEE MTT-S). He is also a member of the Technical Committees of the European Microwave Conference (EuMC) and International Congress on Advanced Electromagnetic Materials in Microwaves and Optics (Metamaterials). He serves or has served as a member of the Editorial Board for *IET Microwaves*, *Antennas and Propagation*, *International Journal of RF and Microwave Computer-Aided Engineering*, and *Sensors*. Among his distinctions, he has received the 2006 Duran Farell Prize for Technological Research, holds the Parc de Recerca UAB–Santander Technology Transfer Chair. He was a recipient of three ICREA ACADEMIA Awards (calls 2008, 2013, and 2018). He is a Reviewer of the IEEE TRANSACTIONS ON MICROWAVE THEORY AND TECHNIQUES and the IEEE MICROWAVE AND WIRELESS COMPONENTS LETTERS, among many other journals.